

# Common-path multimodal optical microscopy

Chandra S. Yelleswarapu,<sup>1</sup> Marla Tipping,<sup>2</sup> Sri-Rajasekhar Kothapalli,<sup>1,3</sup>  
Alexey Veraksa,<sup>2</sup> and D. V. G. L. N. Rao<sup>1,\*</sup>

<sup>1</sup>Department of Physics, University of Massachusetts, 100 Morrissey Boulevard, Boston, Massachusetts 02125, USA

<sup>2</sup>Department of Biology, University of Massachusetts, 100 Morrissey Boulevard,  
Boston, Massachusetts 02125, USA

<sup>3</sup>Present address: Department of Biomedical Engineering, Washington University, One Brookings Drive,  
St. Louis, Missouri 63130, USA

\*Corresponding author: raod@umb.edu

Received November 20, 2008; revised March 6, 2009; accepted March 16, 2009;  
posted March 19, 2009 (Doc. ID 104337); published April 10, 2009

We have developed a common-path multimodal optical microscopy system that is capable of using a single optical source and a single camera to image amplitude, phase, and fluorescence features of a biological specimen. This is achieved by varying either contrast enhancement filters at the Fourier plane and/or neutral density/fluorescence filters in front of the CCD camera. The feasibility of the technique is demonstrated by obtaining brightfield, fluorescence, phase-contrast, spatially filtered, brightfield+fluorescence, phase+fluorescence, and edge-enhanced+fluorescence images of the same *Drosophila* embryo without the need for image registration and fusion. This comprehensive microscope has the capability of providing both structural and functional information and may be used for applications such as studying live-cell dynamics and in high throughput microscopy and automated microscopy. © 2009 Optical Society of America  
OCIS codes: 180.0180, 070.0070, 070.6110, 110.0180, 110.4190, 120.3890.

Investigation of complex biological processes requires the imaging of different features of biological specimens. Several optical imaging modalities were developed in the past to observe amplitude and phase differences contained in a specimen [1–3]. Furthermore, fluorophore labeling can be used to identify specific features of interest. While brightfield, amplitude, and phase-based imaging techniques primarily reveal morphological information, fluorescence imaging can reveal functional information of live cells. The use of lasers as light sources has considerably expanded the boundaries of optical imaging [4–11]. It is possible to obtain comprehensive information about the specimen by combining different optical imaging modalities (such as phase-based contrast enhancement, fluorescence, or nonlinear optical properties) [10–13]. At present it is common practice to apply two or more of these different imaging modalities one after the other and to digitally register the resulting images together for structural and/or functional information. In most cases such a procedure utilizes multiple geometries—fluorescence imaging in reflection geometry and contrast-enhancement-based imaging in transmission geometry. This requires switching between the light sources and the associated optical paths and hence makes it difficult to image some biological events that occur at very short time scales. Therefore the use of different microscope geometries for multimodal imaging is not an ideal choice for applications such as the study of live-cell dynamics or high-throughput microscopy. For such applications, it would be beneficial to image all the details contained in the specimen at once, without the necessity of any digital image registration and fusion.

We report a novel common-path multimodal optical microscopy (CMOM) technique where the absorption,

phase, and fluorescence features of biological specimens are imaged using a single optical source. To switch between different modalities, the only requirement is to replace the contrast enhancement filters at the Fourier plane and the neutral density/fluorescence filters in front of the CCD camera. Moreover, by using a laser-line notch filter (NF), the bright-field+fluorescence, phase+fluorescence, and edge-enhanced+fluorescence features of the *Drosophila* embryo are imaged at once without the need for digital-image registration and fusion.

The CMOM setup is based on a typical transmission light microscope, with the addition of a 4-*f* imaging system, as shown in Fig. 1a. The specimen is illuminated by a well-collimated 488 nm wavelength line of the Ar–Kr laser. An input power of ~20 mW is used in all our experiments. A microscope objective (Nikon CFI 60 infinity-corrected brightfield objective, 10×, 0.3 NA) collects light from the specimen and is collimated using lens L<sub>1</sub>. Two 20 cm focal length lenses (L<sub>2</sub> and L<sub>3</sub>) are arranged in the 4-*f* geometry to perform the Fourier and inverse Fourier transforms, and the object is imaged on the CCD camera placed at the backfocal plane of lens L<sub>3</sub>.

A bright-field image of a *Drosophila* embryo, obtained using the CMOM system without any filters at the Fourier plane or in front of the CCD camera, is shown in Fig. 1b. As would be expected, the internal features of the embryo are not clearly visible. For phase-contrast imaging, we first modified the CMOM to a Fourier phase-contrast microscope (FPCM) by inserting a phase filter (a dye-doped twisted nematic liquid crystal, LC) at the Fourier plane (F<sub>1</sub>) [6]. It is well known that when a collimated laser beam bearing object information is focused with a converging lens, the pattern obtained at the backfocal plane is analogous to the Fourier transformation of the object

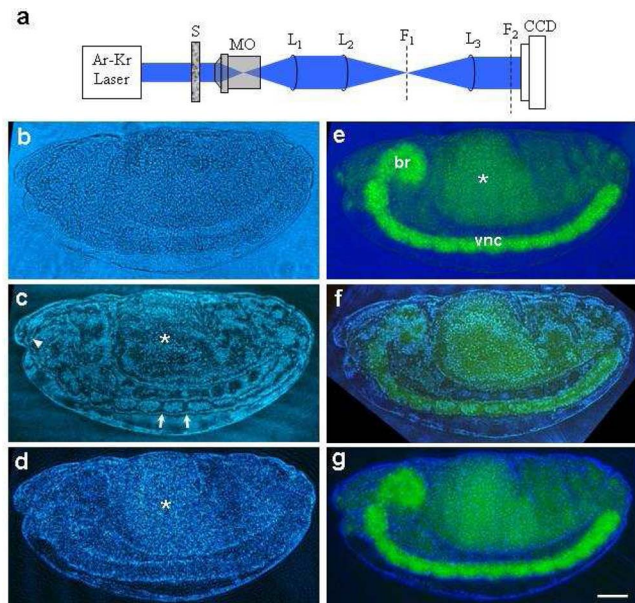


Fig. 1. (Color online) CMOM system and its application in imaging amplitude, phase, and fluorescence features of a *Drosophila* embryo. All panels show the same embryo, stained with antielav primary antibody to visualize the nervous system, followed by FITC-conjugated secondary antibody. Scale bar, 50  $\mu\text{m}$ . a, Schematic of the experimental setup. S, sample; MO, microscope objective; L, lens;  $F_1$ , Fourier plane;  $F_2$ , filter plane. b, Conventional bright-field image. Internal structures of the embryo are not well defined. c, FPCM image obtained using a phase filter at  $F_1$  and neutral density filter (NDF) at  $F_2$ . Segmental boundaries are clearly visible in this sagittal image (arrows) as well as the invaginating foregut primordia at the stomodeum (arrowhead), the midgut area (asterisk), and other internal features. d, Edge-enhanced image obtained with a high-pass spatial filter at  $F_1$  and NDF at  $F_2$ . Inner yolk-containing cells are optically dense and appear as a lighter area in the middle of the embryo (asterisk). e, Fluorescence image with laser line notch filter (NF) at  $F_2$  and no filter at  $F_1$ . The segmented ventral nerve cord (vnc) and the brain region (br) are detected in the sagittal optical section of the embryo. Although the NF blocks most of the excitation source, a small amount of light leaks through, making it possible to observe the overall embryo morphology. The midgut is autofluorescent (asterisk). f, Phase + fluorescence image obtained with a phase filter at  $F_1$  and NF at  $F_2$ . Both the FPCM and trans-fluorescence information are recorded at the same time. Most of the information visible in part c is retained, with the nervous system and midgut fluorescence also detectable. g, Edge-enhanced + fluorescence image obtained with a spatial filter at  $F_1$  and NF at  $F_2$ . The boundary of the embryo is better resolved (compare to e), and the fluorescence signal is clearly visible.

information [14]. Generally the Fourier spectrum contains low spatial frequencies with high intensities at the center and high spatial frequencies with low intensities on the edges. When the LC cell is placed at  $F_1$ , high-intensity, low spatial frequencies induce local LC molecules into the isotropic phase, whereas low-intensity, high spatial frequencies at the edges are not intense enough, and hence the molecules in this region remain in an anisotropic phase. Since only aligned LC molecules (anisotropic phase) impose

an amount of phase to the incident light wave as it passes through, high spatial frequencies acquire an additional  $\pi/2$  of a wavelength phase change. However, the low spatial frequencies transmit through the self-induced isotropic phase of the LC cell without acquiring any phase difference. This leads to a relative phase difference of  $\pi/2$  between these two light beams, the primary criterion for phase-contrast imaging, at the exit plane of the LC cell. Thus by simply placing the LC cell at the Fourier plane  $F_1$ , the CMOM system can be modified into an FPCM. As shown in Figure 1c, the resulting FPCM image of the same *Drosophila* embryo displays high contrast, with several clearly visible distinct features such as segmental boundaries (arrows), the anterior mouth opening, or stomodeum (arrowhead), the midgut (asterisk), as well as other internal structures.

To image amplitude related features, the phase filter at the Fourier plane  $F_1$  is replaced with an amplitude filter (spatial filter)—an opaque dot on the microscope cover glass. When the opaque dot is spatially overlapped with the center of the Fourier spectrum, low spatial frequencies are blocked, while the remaining high spatial frequency components are imaged onto the CCD camera. Figure 1d shows high pass filtering where the structural features of the embryo are clearly visible. The most prominent structure observable in this image is the midgut, which contains optically dense cells (seen as a lighter mass in the middle of the embryo, asterisk). The higher optical density of this region is presumably due to the high concentration of yolk proteins and lipids in these cells [15]. Other internal structures are also visible, such as a part of the ventral nerve cord, and the overall boundary of the embryo is distinguishable from the background. Spatial filtering can therefore highlight optically dense regions in the specimen, which are difficult to observe with other modalities. Thus the addition of the  $4-f$  geometry to the transmission-light microscope makes it possible to image both amplitude and phase features of the specimen simply by changing contrast-enhancement filters at the Fourier plane.

Transfluorescence imaging was pioneered prior to introduction of epifluorescence. However, it was abandoned thereafter largely due to the unavailability of good fluorescence filters that could efficiently block the excitation light from reaching the CCD camera. With the advent of new filter technology, transfluorescence imaging should not suffer from the disadvantage of an incompletely blocked excitation source [16]. In the CMOM system, owing to transfluorescence imaging, both the excitation source and fluorescence emission signal reach the CCD camera. Because the excitation power far exceeds the emission power, the excitation source normally has to be blocked by using an emission filter. Instead, we used an NF (Semrock NF01-488U-25) to reduce the excitation source power without blocking it completely so that it is comparable to the fluorescence emission. This reduction enabled us to obtain hybrid images such as brightfield+fluorescence, phase + fluorescence, and edge-enhanced+fluorescence



without the need for image registration and merging. At plane  $F_2$  of Fig. 1a, we replaced the emission filter with an NF ( $\sim 6$  OD at 488 nm). The NF orientation (tilt) is adjusted for optimizing the image contrast. It blocked most of the excitation light while transmitting all the other wavelengths with practically no attenuation. Thus both the structure of the embryo and the fluorescence emission are imaged at the same time, as shown in Fig. 1e. The embryo was stained with the anti-elav primary antibody that recognizes all neurons in the central and peripheral nervous system [17], followed by FITC-conjugated secondary antibody. In the sagittal optical section shown in Fig. 1e, the central nervous system of the embryo is clearly visible, with distinct segmented ventral nerve cord and brain regions. Note that the cells in the midgut are autofluorescent (asterisk). The NF allowed us to visualize the overall outline of the embryo, comparable to the brightfield image shown in Fig. 1b. This ability to observe fluorescence against the outline of cells or tissues can be useful in real-time studies of cell dynamics.

To observe phase+fluorescence features, the phase filter is inserted at plane  $F_1$  (while retaining NF at plane  $F_2$ ) of the fluorescence setup. Using this setup, as shown in Fig. 1f, we recorded the phase and fluorescence features of the same *Drosophila* embryo at once. All the structures recognized in the FPCM-only image [Fig. 1c] are present in this combined view, with the added advantage of observing the fluorescence from the nervous system. The fluorescence part of the image recording is not hindered by the presence of the phase filter, because the CCD will record only the changes in the amplitude (intensity) and not the phase. So even if the phase filter induces a  $\pi/2$  phase for the fluorescence light, the fluorescence image is unperturbed. On the other hand, the phase filter will add the required additional  $\pi/2$  phase to the phase information carrying beam and thereby convert the phase variations into the amplitude contrast. Thus we were able to record the coregistered phase and fluorescence information at the same time with a good signal-to-noise ratio. Similarly, Fig. 1g shows an edge-enhanced+fluorescence image in which a spatial filter replaced the phase filter at  $F_1$ . In addition to fluorescence features, the boundary of the embryo and other amplitude related features are clearly enhanced in this combined image, compared to the brightfield+fluorescence mode (compare Figs. 1g and 1e). Again, the presence of a spatial filter did not affect the fluorescence details in the image. Normally the spatial filter is precisely positioned at the Fourier plane for manipulation of respective spatial frequency bands. However, a Fourier plane for an incoherent light source (fluorescent light) cannot be localized as precisely as for a monochromatic light source. Therefore the imaging of fluorescence features of the specimen is not affected by the presence of the spatial filter at the Fourier plane  $F_1$ . Thus this relatively simple multimodal imaging system has the ability to record all the features of a biological speci-

men without switching optical paths, thus obviating the need to perform acquisition of separate images followed by image registration and merging. Using appropriate filters, it will be possible to perform multispectral imaging and to obtain phase and functional information at the same time.

In conclusion, we have developed a CMOM system that can image amplitude, phase, and fluorescence features of a biological specimen at once. To switch between different modalities, it is necessary only to replace the contrast-enhancement filters at the Fourier plane and neutral density/fluorescence filters in front of the CCD camera. Although we demonstrated the feasibility of the system by exploiting Fourier phase-contrast microscopy and conventional spatial filtering, in principle any other real-time phase-based contrast enhancement and spatial filtering techniques can be incorporated. In addition, it may be possible to incorporate other imaging modalities such as Schlieren, two-photon, second-harmonic, and Raman microscopy imaging into this microscopy system. This comprehensive microscope has the capability of simultaneously providing both structural and functional information of biological specimens in a streamlined simplified design with a single optical path. It can potentially be used in high-throughput screening and automated microscopy, where acquisition of the transmitted light image has been of limited use.

## References

1. F. Zernike, *Science* **121**, 345 (1955).
2. G. Nomarski, *J. Phys. Radium* **16**, 9 (1955).
3. J. W. Lichtman and J. Conchello, *Nat. Methods* **2**, 910 (2005).
4. D. J. Stephens and V. J. Allan, *Science* **300**, 82 (2003).
5. S. Fürhapter, A. Jesacher, S. Bernet, and M. Ritsch-Marte, *Opt. Express* **13**, 689 (2005).
6. C. S. Yelleswarapu, S.-R. Kothapalli, Y. R. Vaillancourt, F. J. Aranda, B. R. Kimball, and D. V. G. L. N. Rao, *Appl. Phys. Lett.* **89**, 211116 (2006).
7. P. S. P. Thong, K. W. Kho, W. Zheng, M. Harris, K. C. Soo, and M. Olivo, *J. Mech. Med. Bio.* **7**, 11 (2007).
8. H. Kawano, T. Kogure, Y. Abe, H. Mizuno, and A. Miyawaki, *Nat. Methods* **5**, 373 (2008).
9. T. B. Huff, Y. Shi, Y. Fu, H. Wang, and J.-X. Cheng, *IEEE J. Sel. Top. Quantum Electron.* **14**, 4 (2008).
10. W. C. Warger 2nd, G. S. Laevsky, D. J. Townsend, M. Rajadhyaksha, and C. A. DiMarzio, *J. Biomed. Opt.* **12**, 044006 (2007).
11. J. A. Palero, H. S. de Bruijn, A. P. Heuvel, H. J. C. M. Sterenborg, and H. C. Gerritsen, *Biophys. J.* **93**, 992 (2007).
12. Y. Park, G. Popescu, K. Badizadegan, R. R. Dasari, and M. S. Feld, *Opt. Express* **14**, 8263 (2006).
13. W. J. Cottrell, J. D. Wilson, and T. H. Foster, *Opt. Lett.* **32**, 2348 (2007).
14. J. W. Goodman, *Opt. Photonics News* **2**, 11 (1991).
15. J. A. Campos-Ortega and V. Hartenstein, *The Embryonic Development of Drosophila Melanogaster* (Springer-Verlag, 1985).
16. P. T. Tran and F. Chang, *Biol. Bull.* **201**, 253 (2001).
17. E. M. O'Neill, I. Rebay, R. Tijan, and G. M. Rubin, *Cell* **78**, 137 (1994).